MNIST classification using Neuromorphic Nanowire Networks

Ruomin Zhu
Alon Loeffler
Joel Hochstetter
School of Physics,
The University of Sydney
Sydney, NSW, Australia
rzhu0837@uni.sydney.edu.au
aloe8475@uni.sydney.edu.au
jhoc2571@uni.sydney.edu.au

Adrian Diaz-Alvarez
Tomonobu Nakayama*†
International Center for Materials
Nanoarchitectonics (WPI-MANA),
National Institute for Materials
Science (NIMS)
Tsukuba, Japan
diazalvarez.adrian@nims.go.jp
nakayama.tomonobu@nims.go.jp

Adam Stieg
International Center for Materials
Nanoarchitectonics (WPI-MANA),
National Institute for Materials
Science (NIMS)
Tsukuba, Japan
stieg@cnsi.ucla.edu

James Gimzewski‡‡
University of California, Los Angeles,
California NanoSystems Institute
Los Angeles, CA, USA
gimzewski@cnsi.ucla.edu

Joseph T. Lizier
Faculty of Engineering and Centre for
Complex Systems,
The University of Sydney
Sydney, NSW, Australia
joseph.lizier@sydney.edu.au

Zdenka Kuncic*
School of Physics and
Sydney Nano Institute,
The University of Sydney
Sydney, NSW, Australia
zdenka.kuncic@sydney.edu.au

ABSTRACT

Neuromorphic Nanowire Networks (NWNs) are a novel class of information processing hardware devices, combining the advantage of memristive cross-point junctions and neural-like complex network topology. In addition to their low operating power, NWNs are also easy to fabricate with bottom-up self-assembly. Here, we implement the MNIST handwritten digit classification task on simulated NWNs to demonstrate their ability to perform complex learning tasks. Using a CNN-inspired kernel method and a reservoir computing framework, our simulation results attain an accuracy of nearly 98%. Moreover, this is achieved using only a fraction of the total MNIST training data and without requiring hardware accelerators. We also investigate the information theoretic metrics of mutual information (MI), transfer entropy (TE) and active information storage (AIS) to analyze the MNIST learning dynamics of NWNs. We find that MI with respect to classes is maximized after network feature extraction and that TE is largest when MNIST digit boundaries are processed, while AIS is strongest when areas with lower pixel values are presented. Overall, these results suggest the information processing capabilities of neuromorphic NWNs make them promising candidates for complex learning applications.

CCS CONCEPTS

• **Computing methodologies** → **Artificial intelligence**; **Neural networks**; **Supervised learning by classification**.

KEYWORDS

nanowire networks, neuromorphic, MNIST, kernel, information dynamics, transfer entropy, active information storage

ACM Reference Format:
Ruomin Zhu, Alon Loeffler, Joel Hochstetter, Adrian Diaz-Alvarez, Tomonobu Nakayama, Adam Stieg, James Gimzewski, Joseph T. Lizier, and Zdenka Kuncic. 2021. MNIST classification using Neuromorphic Nanowire Networks. In *International Conference on Neuromorphic Systems 2021 (ICONS 2021), July 27–29, 2021, Knoxville, TN, USA.* ACM, New York, NY, USA, 4 pages. https://doi.org/10.1145/3477145.3477162

1 INTRODUCTION

This study concerns a specific class of memristive neuromorphic systems constructed using bottom-up self-assembly: nanowire networks (NWNs) [13]. Neuromorphic NWNs are disordered systems comprised of passivated metallic nanowires that self-assemble to form a complex network topology with memristive cross-point junctions [2, 24]. Previous studies have demonstrated that NWNs exhibit complex, neural network-like structural properties including small-worldness, modularity and recurrent feedback loops [18]. In response to external stimuli, NWNs exhibit emergent collective dynamics [1, 2, 6, 19–21, 24], which have been shown to be essential for information processing in these neuromorphic devices [2, 5, 15, 21].

Simulation studies of NWNs have demonstrated learning ability under a reservoir computing framework, in which only the readout layer is trained and the network self-adjusts its synapse-like memristive junctions. Moreover, the computing resources within NWNs can be utilized most efficiently when the input is time-dependent [1, 7, 11, 24, 26]. The MNIST handwritten digit classification task has become the "hello world" in the field of machine learning [14].

*Also with Graduate School of Pure and Applied Sciences, University of Tsukuba.
†Also with School of Physics, The University of Sydney.
‡Also with International Center for Materials Nanoarchitectonics (WPI-MANA), National Institute for Materials Science (NIMS).

ICONS 2021, July 27–29, 2021, Knoxville, TN, USA

ACM ISBN 978-1-4503-8691-3/21/07…$15.00
https://doi.org/10.1145/3477145.3477162

Here, we convert the original MNIST dataset to temporal streams via a shifting kernel and test the performance of NWNs on this task as a benchmark. Furthermore, we use information-theoretic measures to investigate the dynamics within NWNs while learning MNIST digits, to gain deeper insight into the information processing capability of these neuromorphic systems.

2 METHODS

We use a physically motivated model (detailed elsewhere [10–12]) to simulate the MNIST classification task implemented on NWNs under a reservoir computing framework. The MNIST dataset is pre-processed and delivered to NWNs temporally to utilize the signal processing capacity of the recurrent memristive network [7]. The training set used in this study is comprised of a randomly selected subset of the original MNIST training dataset. The entire MNIST testing dataset is employed and shuffled to test the classification accuracy. A kernel method inspired by convolutional neural networks [8, 14] is applied to convert the original MNIST image pixel values to temporal input signals delivered to the network.

2.1 Kernel scanning

MNIST images are pre-processed with a shifting kernel of size $\kappa \times \kappa$ and duration $\Delta t = 1$ s to extract features. The traverse of the kernel starts from the top left corner of the image, moving horizontally with a stride of 1 pixel at each Δt until its right boundary reaches the last column of the image. The kernel then moves back to the left most column and shifts one row down from the original position. Fig. 1 illustrates this method for a kernel with $\kappa = 5$. Each MNIST image (comprised of 28×28 pixels) is scanned by the kernel $(29-\kappa)^2$ times in total, and the features re-arranged into a 2D shape as shown in fig. 1c. At each Δt, the kernel pixel values (fig. 1b) are converted into normalised voltages and delivered to dedicated input electrodes in the network (fig. 1d).

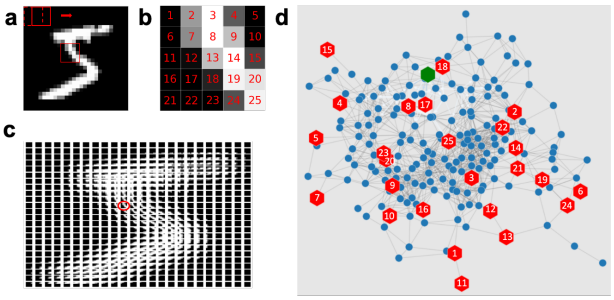

Figure 1: Schematic illustration of the kernel scanning method. Each MNIST image (a) is scanned by a kernel (size 5×5 shown here) (b) that shifts by 1 pixel, thus creating a 2D feature representation (c). Kernel pixel intensities are converted to voltage signals which are (d) input to the network temporally via dedicated electrodes (25 in this case) over a duration of 1 s per kernel pixel.

The role of the network is to project features into a higher dimensional space such that they become linearly separable. Currents on the κ^2 input electrodes are read simultaneously as the input voltages are delivered. Through the learning period of each MNIST image, every electrode has $(29-\kappa)^2$ readouts, with Δt duration of each readout. The final readout is recorded for each scan of period Δt for each electrode, and re-arranged into κ^2 2D matrices of shape $I_{(29-\kappa)\times(29-\kappa)}$, as shown in fig. 2a. The most salient features are then extracted by taking the maximum of I in each row and column, as shown in fig. 2b:

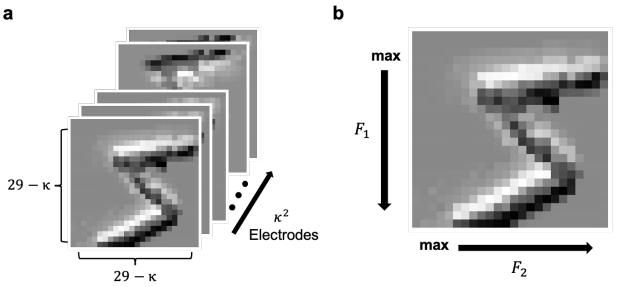

Figure 2: Schematic illustration of feature extraction. (a) During the learning period of each MNIST image, current on κ^2 input electrodes is recorded and re-arranged into 2D matrices $I_{(29-\kappa)\times(29-\kappa)}$. (b) For each electrode, features are sampled as max values along each column (F_1) and each row (F_2).

$$F_i = \max(I, \text{axis} = i), \qquad i = 1, 2 \tag{1}$$

where F_1 and F_2 are both of length $29-\kappa$ for each electrode. As a result, $2 \times (29-\kappa)$ salient features are obtained from each electrode, giving a total of $2\kappa^2(29-\kappa)$ features per each MNIST image. Linear discriminant analysis (LDA) is then employed to classify the digits based on these features.

2.2 Information Dynamics

In addition to demonstrating the system's learning capability via MNIST classification, its performance can be related to an intrinsic information processing capability. We focus on the information theoretic measures of mutual information (MI), transfer entropy (TE) and active information storage (AIS), which provide insights into the intrinsic information transfer and storage of complex networks [4, 16, 17, 22], and a way to analyze the dynamics of a network (e.g. recurrent neural network [3]) during learning.

MI estimates the relative information between system variables [9, 23]. In this work, features at different stages are binarized and thresholded to maximize MI. MI is estimated at different stages of the algorithm (i.e. MNIST pixel values, kernel scanned data, features extracted from the network) to determine the influence of each step (details can be found in previous work [23]). TE quantifies the amount of information provided by the past activity of a source component in predicting the target component's state, and captures directed information flow between these components [4, 22]. In the context of networks, information transfer is calculated between connected nodes [16, 25]. Transfer entropy from node i to node j is calculated as the mutual information from the past of voltage time series i, $\mathbf{V}_i(n)$, to that of j, $\mathbf{V}_j(n+1)$, conditioned on the past k values of j, $\mathbf{V}_j^k(n)$: $\mathbf{TE}_{i,j} = I\left(\mathbf{V}_i(n); \mathbf{V}_j(n+1) | \mathbf{V}_j(n)\right)$. For the edge e connecting nodes i and j, TE is calculated in both directions:

$\mathbf{TE}_e = \mathbf{TE}_{i,j} + \mathbf{TE}_{j,i}$. AIS quantifies the amount of information provided by a component's past activity about its own state update, capturing the active memory for computing its next value [17]. In NWNs, memory is incorporated by the conductance on junctions (edges). Active information storage is thereby calculated based on the conductance time-series $\mathbf{G_e}(n)$ of junctions e [16, 25], as the mutual information from the past k values of the conductance $\mathbf{G_e}^k(n)$ to the next value $G_e(n+1)$: $\mathbf{AIS}_e = I\left(\mathbf{G_e}^k(n); G_e(n+1)\right)$. In this study, TE and AIS are estimated (using the JIDT software [16]) for each Δt period with correspondence to the kernel scans described in fig. 1 and averaged across the network.

3 RESULTS

3.1 MNIST classification

Figure. 3 (a) shows MNIST classification accuracy with respect to the number of samples in the training group, using a kernel with $\kappa = 5$. Classification accuracy increases as more training samples are used, until saturating at $\approx$ 96.2%. Fig. 3 (b) shows the accuracy as a function of κ. Here, both training and testing groups are composed of 10,000 MNIST images. This figure only includes results for $3 \leq \kappa \leq 13$ due to the limitation of network size. When $\kappa = 1$, the kernel delivers data to the network one pixel at a time from the original image, without generating richer features from combinations of neighboring pixels, and there are insufficient features ($2\kappa^2(29 - \kappa) = 56$) to perform classification with high accuracy. On the other hand, when $\kappa = 28$, the kernel delivers the whole image into the system at once. While this process results in many features, the entire image is delivered over Δt, resulting in loss of detail due to the short duration. This makes it impossible to identify the digit. Fig. 3 (b) demonstrates that the accuracy saturates to $\approx$ 97.8% as κ increases, with $\kappa = 9$ being the optimal size of the kernel. At this size, enough features are extracted without losing too many details over the learning period.

The MNIST classification task has been a common benchmark for all types of neural networks and learning algorithms. CNNs have demonstrated an unparalleled accuracy of over 99% while other ANNs are able to achieve an accuracy ranging between 95.3% to 98.4% [14]. These methods require multiple fully connected layers and numerous learning epochs and are thus computationally intensive. Here, a comparable accuracy is achieved by employing a recurrent network with sparse connectivity under the reservoir computing framework. More importantly, these simulation results suggest that NWNs can achieve high classification accuracy using only $\approx$ 10% of the MNIST training dataset. Furthermore, as all the learning can be accomplished in a single epoch using only CPUs, NWNs are also less computationally intensive than ANNs.

3.2 Information dynamics

Table 1 lists the MI (natural logarithm) between each MNIST digit class (in 10,000 samples) and the data at different stages. MI increases with each stage of the algorithm and exhibits a marked increase when the most salient features are extracted from the network readouts by Eq. 1, indicating significant learning progress. Applying the same feature selection to the kernel scans (without network processing) results in substantially lower MI of 0.122 nats.

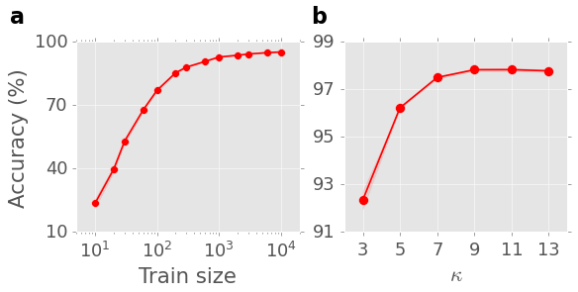

Figure 3: (a) Classification accuracy as a function of number of MNIST images used for training for a kernel size $\kappa = 5$. (b) Classification accuracy as a function of kernel size.

Fig. 4 shows examples of the dynamical information theoretic measures within the neuromorphic system when learning the digits "0" (Fig. 4a-c) and "9" (Fig. 4d-f). Fig. 4a,d show the mean of input kernels across different instances of "0" and "9". These are obtained by selecting out each instance of each digit from the whole time series and then averaging the pixel values within the kernel scans (cf. fig. 1b), and then across instances. Intrinsic information dynamics is then estimated at each Δt with correspondence to kernel scans.

Table 1: Mutual Information (nats) with Class

Raw	Scanned	Selected Input	Readout	Features
0.0877	0.115	0.122	0.123	0.163

Fig. 4b,e show TE averaged across instances of "0" and "9" and rearranged into the same shape as fig. 4a. These results suggest that information transfer is strongest when the kernel traverses across the horizontal edge of a digit (i.e. TE acts like an edge detector). Input signals delivered from these areas tend to be substantially different from their values in the previous kernel scan, and so drive more complex transient dynamics in the system, hence inducing stronger information flow between the nodes in the network. Similarly, fig. 4c,f show AIS when learning "0" and "9". In contrast to TE, these results indicate that the network exhibits stronger AIS when the kernel traverses areas with lower pixel values. The network tends to remain in similar stationary states at these points, where its memory of past states dominates the dynamics.

4 CONCLUSIONS

Neuromorphic nanowire networks represent a novel approach for neuro-inspired computing and information processing. In this study, the CNN-inspired kernel method applied to pre-process the MNIST dataset enabled NWNs to achieve an overall high performance on this classification task when implemented in a reservoir computing framework. An accuracy comparable to ANNs can be achieved using less training data and less computing resources. Additionally, information theoretic analysis of NWNs during MNIST learning demonstrated substantially increased mutual information between the extracted features and the classes, compared to raw data and classes. Furthermore, information transfer is maximised near the

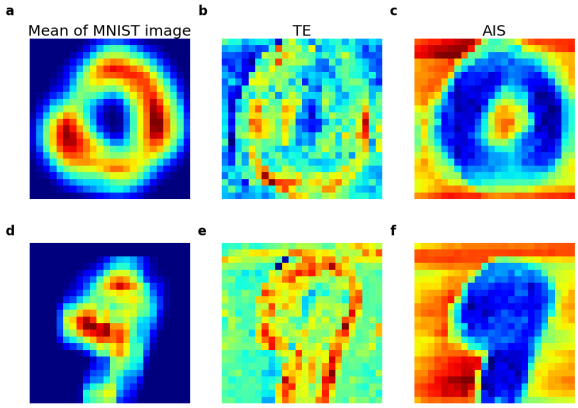

Figure 4: Information dynamics of learning the digits "0" and "9". (a) Average pixel values within the kernel for digit "0"; (b) Corresponding average TE across the network; (c) Corresponding average AIS across the network. (d)-(f) Same as (a)-(c) except for the digit "9". For each digit, all three figures are averaged across different learning periods.

digit boundaries, while information storage is maximised in regions of lower pixel values. These proof-of-principle simulation results demonstrate the potential of nanowire networks for neuromorphic information processing and provide a useful scheme for hardware implementation of the MNIST classification task as well as more complex dynamical classification tasks such as human action recognition.

ACKNOWLEDGMENTS

The authors acknowledge the Artemis HPC resource at the Sydney Informatics Hub. R.Z. is supported by the PREA scholarship from the University of Sydney. J.H. and A.L. are supported by the RTP scholarship from the University of Sydney.

REFERENCES

[1] Audrius V. Avizienis, Henry O. Sillin, Cristina Martin-Olmos, Hsien Hang Shieh, Masakazu Aono, Adam Z. Stieg, and James K. Gimzewski. 2012. Neuromorphic Atomic Switch Networks. *PLoS ONE* 7, 8 (2012), e42772. https://doi.org/10.1371/journal.pone.0042772

[2] Allen T Bellew, Alan P Bell, Eoin K McCarthy, Jessamyn A Fairfield, and John J Boland. 2014. Programmability of nanowire networks. *Nanoscale* 6, 16 (2014), 9632–9639.

[3] Joschka Boedecker, Oliver Obst, Joseph T. Lizier, N.M. Mayer, and Minoru Asada. 2012. Information processing in echo state networks at the edge of chaos. *Theory in Biosciences* 131, 3 (2012), 205–213. https://doi.org/10.1007/s12064-011-0146-8

[4] Terry Bossomaier, Lionel Barnett, Michael Harré, and Joseph T. Lizier. 2016. *An Introduction to Transfer Entropy: Information Flow in Complex Systems.* Springer International Publishing. https://doi.org/10.1007/978-3-319-43222-9

[5] Adrian Diaz-Alvarez, Rintaro Higuchi, Qiao Li, Yoshitaka Shingaya, and Tomonobu Nakayama. 2020. Associative Routing through Neuromorphic Nanowire Networks. *AIP Advances* 10, 2 (2020), 025134. https://doi.org/10.1063/1.5140579

[6] Adrian Diaz-Alvarez, Rintaro Higuchi, Paula Sanz-Leon, Ido Marcus, Yoshitaka Shingaya, Adam Z. Stieg, James K. Gimzewski, Zdenka Kuncic, and Tomonobu Nakayama. 2019. Emergent Dynamics of Neuromorphic Nanowire Networks. *Scientific Reports* 9, 1 (2019), 14920. https://doi.org/10.1038/s41598-019-51330-6

[7] Kaiwei Fu, Ruomin Zhu, Alon Loeffler, Joel Hochstetter, Adrian Diaz-Alvarez, Adam Stieg, James Gimzewski, Tomonobu Nakayama, and Zdenka Kuncic. 2020. Reservoir Computing with Neuromemristive Nanowire Networks. In *2020 International Joint Conference on Neural Networks (IJCNN).* 1–8. https://doi.org/10.1109/IJCNN48605.2020.9207727

[8] Kunihiko Fukushima and Sei Miyake. 1982. Neocognitron: A self-organizing neural network model for a mechanism of visual pattern recognition. In *Competition and cooperation in neural nets.* Springer, 267–285.

[9] R. Devon Hjelm, Alex Fedorov, Samuel Lavoie-Marchildon, Karan Grewal, Phil Bachman, Adam Trischler, and Yoshua Bengio. 2019. Learning Deep Representations by Mutual Information Estimation and Maximization. *arXiv:1808.06670* (2019).

[10] Joel Hochstetter, Ruomin Zhu, Alon Loeffler, Adrian Diaz-Alvarez, Tomonobu Nakayama, and Zdenka Kuncic. 2021. Avalanches and edge-of-chaos learning in neuromorphic nanowire networks. *Nature Communications* 12, 1 (2021), 1–13. https://doi.org/10.1038/s41467-021-24260-z

[11] Zdenka Kuncic, Omid Kavehei, Ruomin Zhu, Alon Loeffler, Kaiwei Fu, Joel Hochstetter, Mike Li, James M. Shine, Adrian Diaz-Alvarez, Adam Stieg, James Gimzewski, and Tomonobu Nakayama. 2020. Neuromorphic Information Processing with Nanowire Networks. In *2020 IEEE International Symposium on Circuits and Systems (ISCAS).* 1–5. https://doi.org/10.1109/ISCAS45731.2020.9181034

[12] Zdenka Kuncic, Ido Marcus, Paula Sanz-Leon, Rintaro Higuchi, Yoshitaka Shingaya, Ming Li, Adam Stieg, James Gimzewski, Masakazu Aono, and Tomonobu Nakayama. 2018. Emergent Brain-like Complexity from Nanowire Atomic Switch Networks: Towards Neuromorphic Synthetic Intelligence. In *2018 IEEE 18th International Conference on Nanotechnology (IEEE-NANO).* 1–3. https://doi.org/10.1109/NANO.2018.8626236

[13] Zdenka Kuncic and Tomonobu Nakayama. 2021. Neuromorphic nanowire networks: principles, progress and future prospects for neuro-inspired information processing. *Advances in Physics: X* 6, 1 (2021), 1894234.

[14] Yann Lecun, Léon Bottou, Yoshua Bengio, and Patrick Haffner. 1998. Gradient-Based Learning Applied to Document Recognition. *Proc. IEEE* 86, 11 (1998), 2278–2324. https://doi.org/10.1109/5.726791

[15] Qiao Li, Adrian Diaz-Alvarez, Ryo Iguchi, Joel Hochstetter, Alon Loeffler, Ruomin Zhu, Yoshitaka Shingaya, Zdenka Kuncic, Ken-ichi Uchida, and Tomonobu Nakayama. 2020. Dynamic Electrical Pathway Tuning in Neuromorphic Nanowire Networks. *Advanced Functional Materials* 30, 43 (2020), 2003679. https://doi.org/10.1002/adfm.202003679

[16] Joseph T. Lizier. 2014. JIDT: An Information-Theoretic Toolkit for Studying the Dynamics of Complex Systems. *Frontiers in Robotics and AI* 1 (2014). https://doi.org/10.3389/frobt.2014.00011

[17] Joseph T. Lizier, Mikhail Prokopenko, and Albert Y. Zomaya. 2012. Local Measures of Information Storage in Complex Distributed Computation. *Information Sciences* 208 (2012), 39–54. https://doi.org/10.1016/j.ins.2012.04.016

[18] Alon Loeffler, Ruomin Zhu, Joel Hochstetter, Mike Li, Kaiwei Fu, Adrian Diaz-Alvarez, Tomonobu Nakayama, James M. Shine, and Zdenka Kuncic. 2020. Topological Properties of Neuromorphic Nanowire Networks. *Frontiers in Neuroscience* 14 (2020), 184. https://doi.org/10.3389/fnins.2020.00184

[19] Hugh G. Manning, Fabio Niosi, Claudia Gomes da Rocha, Allen T. Bellew, Colin O'Callaghan, Subhajit Biswas, Patrick F. Flowers, Benjamin J. Wiley, Justin D. Holmes, Mauro S. Ferreira, and John J. Boland. 2018. Emergence of Winner-Takes-All Connectivity Paths in Random Nanowire Networks. *Nature Communications* 9, 1 (2018), 3219. https://doi.org/10.1038/s41467-018-05517-6

[20] Gianluca Milano, Giacomo Pedretti, Matteo Fretto, Luca Boarino, Fabio Benfenati, Daniele Ielmini, Ilia Valov, and Carlo Ricciardi. 2020. Brain-Inspired Structural Plasticity through Reweighting and Rewiring in Multi-Terminal Self-Organizing Memristive Nanowire Networks. *Advanced Intelligent Systems* 2, 8 (2020), 2000096. https://doi.org/10.1002/aisy.202000096

[21] Colin O'Callaghan, Claudia G. Rocha, Fabio Niosi, Hugh G. Manning, John J. Boland, and Mauro S. Ferreira. 2018. Collective Capacitive and Memristive Responses in Random Nanowire Networks: Emergence of Critical Connectivity Pathways. *Journal of Applied Physics* 124, 15 (2018), 152118. https://doi.org/10.1063/1.5037817

[22] Thomas Schreiber. 2000. Measuring Information Transfer. *Physical Review Letters* 85, 2 (2000), 4.

[23] James M. Shine, Mike Li, Oluwasanmi Koyejo, Ben Fulcher, and Joseph T. Lizier. 2020. *Topological Augmentation of Latent Information Streams in Feed-Forward Neural Networks.* Preprint. https://doi.org/10.1101/2020.09.30.321679

[24] Adam Z. Stieg, Audrius V. Avizienis, Henry O. Sillin, Cristina Martin-Olmos, Masakazu Aono, and James K. Gimzewski. 2012. Emergent Criticality in Complex Turing B-Type Atomic Switch Networks. *Advanced Materials* 24, 2 (2012), 286–293. https://doi.org/10.1002/adma.201103053

[25] Ruomin Zhu, Joel Hochstetter, Alon Loeffler, Adrian Diaz-Alvarez, Tomonobu Nakayama, Joseph T. Lizier, and Zdenka Kuncic. 2021. Information Dynamics in Neuromorphic Nanowire Networks. *Scientific Reports* 11, 1 (2021), 13047. https://doi.org/10.1038/s41598-021-92170-7

[26] Ruomin Zhu, Joel Hochstetter, Alon Loeffler, Adrian Diaz-Alvarez, Adam Stieg, James Gimzewski, Tomonobu Nakayama, and Zdenka Kuncic. 2020. Harnessing adaptive dynamics in neuro-memristive nanowire networks for transfer learning. In *2020 International Conference on Rebooting Computing (ICRC).* 102–106. https://doi.org/10.1109/ICRC2020.2020.00007